Supporting Information for "The Slab Puzzle of the Alpine-Mediterranean Region: Insights from a new, High-Resolution, Shear-Wave Velocity Model of the Upper Mantle"

A. El-Sharkawy[1,2], T. Meier[1], S. Lebedev[3], J. Behrmann[4], M. Hamada[2], L. Cristiano[5], C. Weidle[1], D. Köhn[1]

[1]Institute of Geosciences, Christian-Albrechts-Universität, Kiel, Germany

[2]National Research Institute of Astronomy and Geophysics (NRIAG), 11421, Helwan, Cairo, Egypt

[3]School of Cosmic Physics, Geophysics Section, Dublin Institute for Advanced Studies, Dublin, Ireland

[4]GEOMAR Helmholtz Centre for Ocean Research, Kiel, Germany.

[5]Deutsches GeoForschungsZentrum (GFZ), Telegrafenberg 14473, Potsdam, Germany.

Contents of this file

1. Introduction

2. Figures S1 to S12

Additional Supporting Information (Files uploaded separately)

1. Table S1: A complete list of the digital object identifiers (DOIs) for all seismic networks used in this study.

—————

Corresponding author: Amr El-Sharkawy, Institute of Geosciences, Christian-Albrechts University, Otto Hahn Platz 1, 24118 Kiel, Germany.(amr.elsharkawy@ifg.uni-kiel.de, amr_elsharkawy22@yahoo.com)

June 15, 2020, 8:18am

Introduction This section provides additional information to further support the obtained results and the 3-D shear-wave velocity model (MeRE2020) as well as the preceding processing steps, following the structure of the main paper. We show all automatically measured inter-station dispersion curves plotted on top of each other as well as the ray-path density. 2-D histogram for the measured phase-velocities as function of frequency as well as for the standard deviations and standard errors as function of both inter-station distance and frequency are also given, respectively. Additional 2-D isotropic phase-velocity maps and their resolution tests are then shown. This is followed by examples of the constructed local dispersion curves at some selected grid nodes. A graphical representation of the parameterization of the background model for the particle swarm optimization inversion (PSO) is shown. Horizontal as well as vertical cross sections through MeRE2020 in comparison with the intermediate-depth seismicity (ISC catalog: 1990 - 2019) are given. Furthermore, we show the depth-dependent uncertainties of the model along the same profiles.
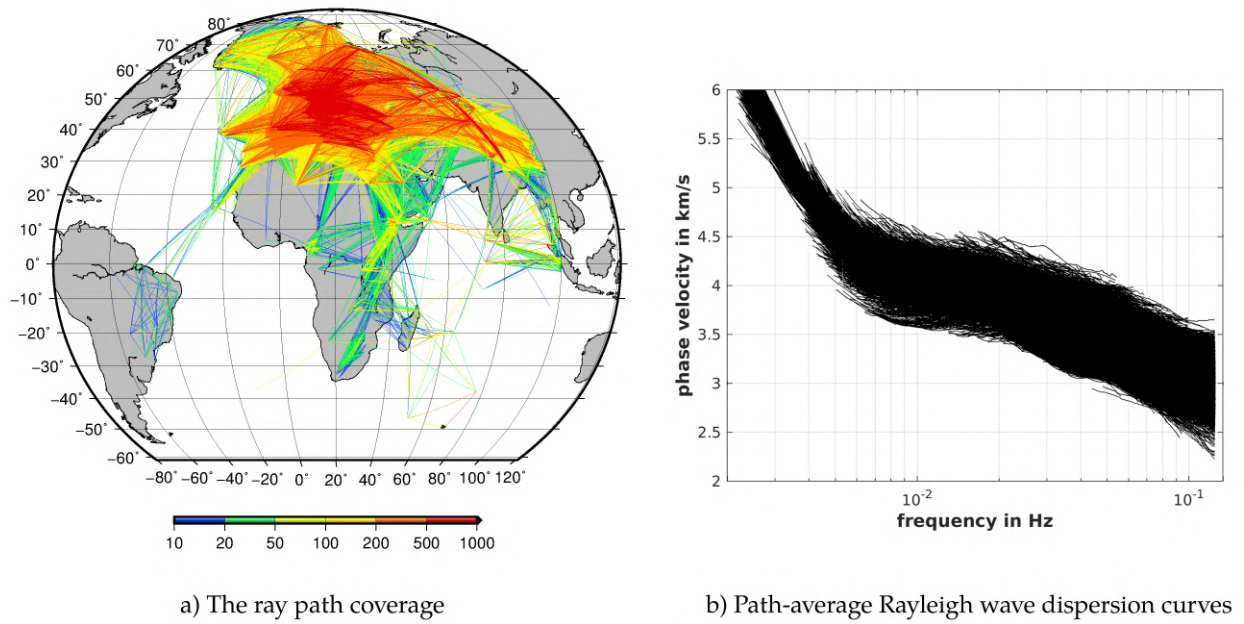
a) The ray path coverage

b) Path-average Rayleigh wave dispersion curves

Figure S1.   a) Color-coded ray-path coverage indicates the number of events recorded by each station-pair on the same great-circle path, b) path-wise averaged Rayleigh-wave phase-velocity measurements (~ 200.000) are plotted on top of each other.
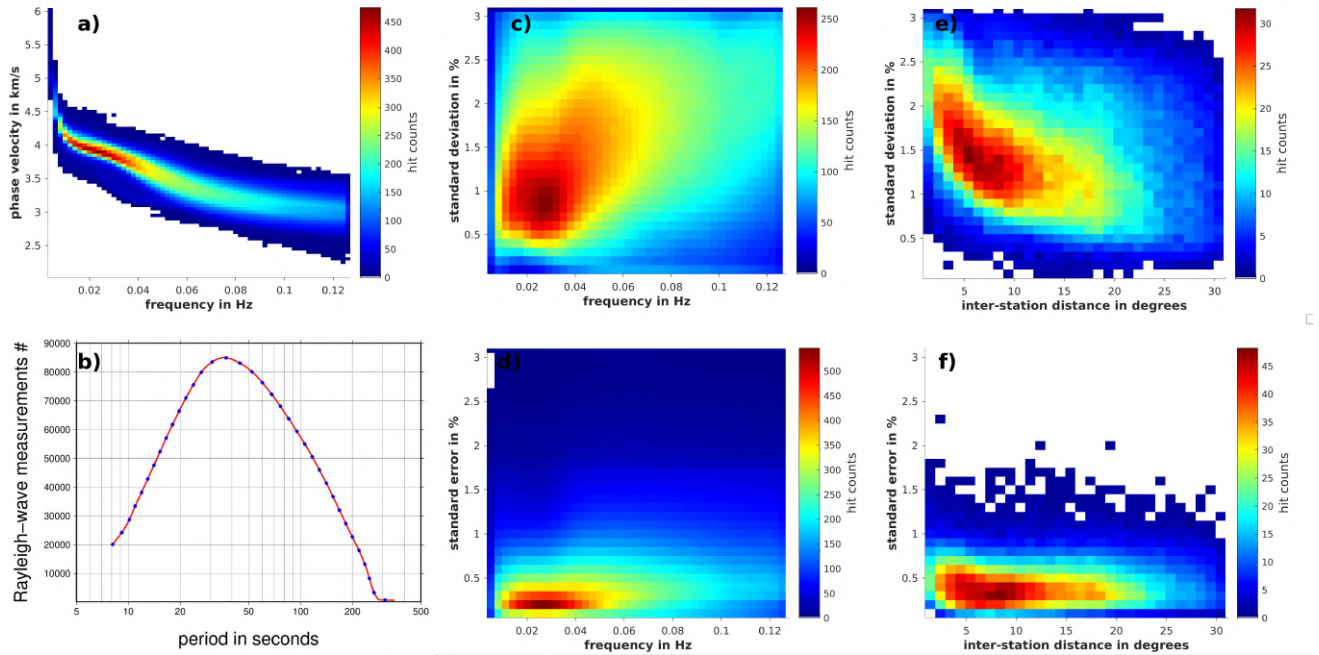
Figure S2.   (a) 2-D histogram of all automatically measured Rayleigh-wave inter-station phase-velocities as function of frequency. (b) Number of Rayleigh-wave measurements as function of period. 2-D histograms of the standard deviations and standard errors as function of frequency as well as the inter-station distance are shown in c, d, e, and f, respectively.
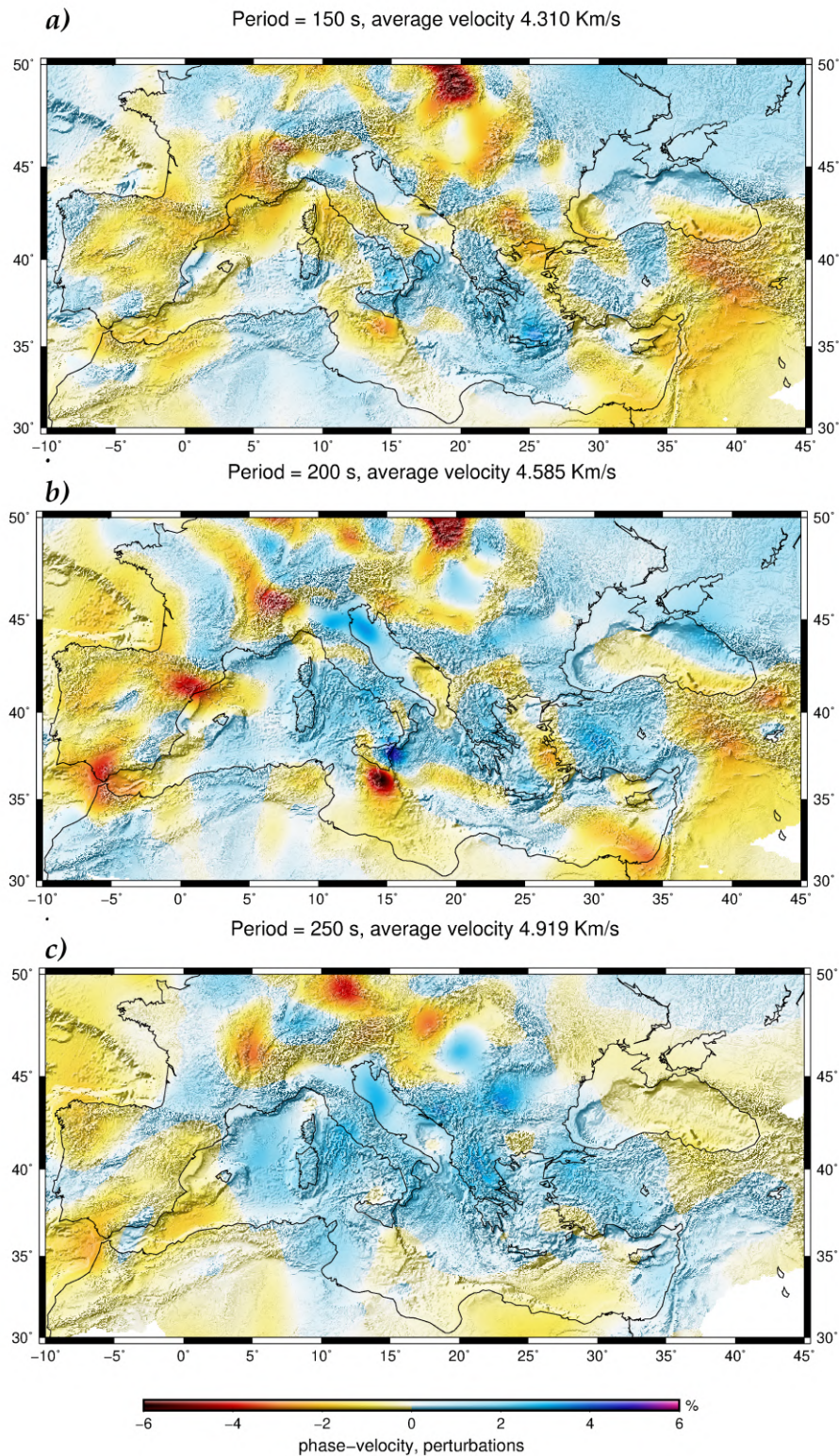
a) Period = 150 s, average velocity 4.310 Km/s

b) Period = 200 s, average velocity 4.585 Km/s

c) Period = 250 s, average velocity 4.919 Km/s

%
phase−velocity, perturbations

Figure S3. Isotropic Rayleigh-wave phas-velocity maps at 150, 200 and 250 s. Perturbations of phase-velocities are plotted relative to the average phase-velocity at the corresponding period given at top of each map.
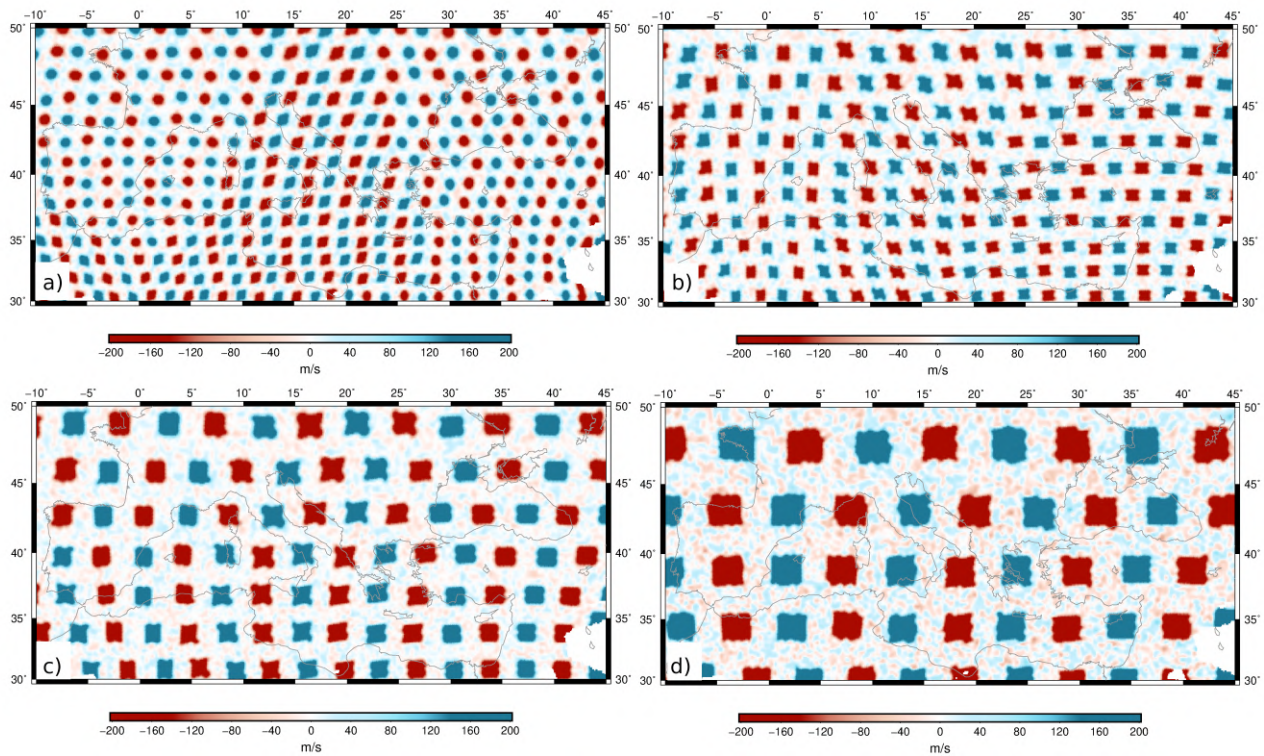
June 15, 2020, 8:18am

Figure S4.   Synthetic checkerboard resolution tests for the Rayleigh-wave phase-velocity. The checkerboard consists of blocks of alternating positive and negative velocity anomalies (± 200 m/s) discretized on block sizes of 75, 100, 150 and 200 km, respectively. Random Guassian noise with a standard deviation of 40 m/s corresponding to 20 % of the checkerboard perturbations has been added to the synthetic data.
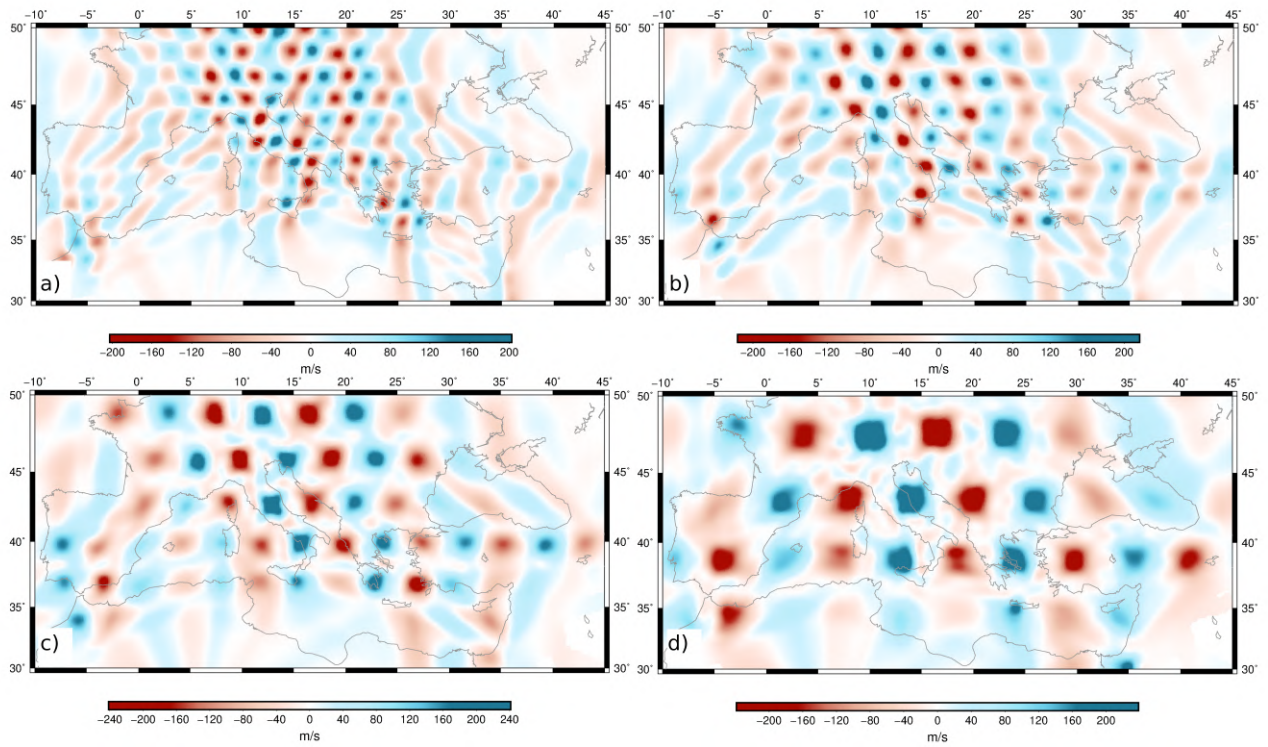
Figure S5. Results of the checkerboard resolution tests at period of 30 s for a) 75 km, b) 100 km, c) 150 km and d) 200 km structure size.
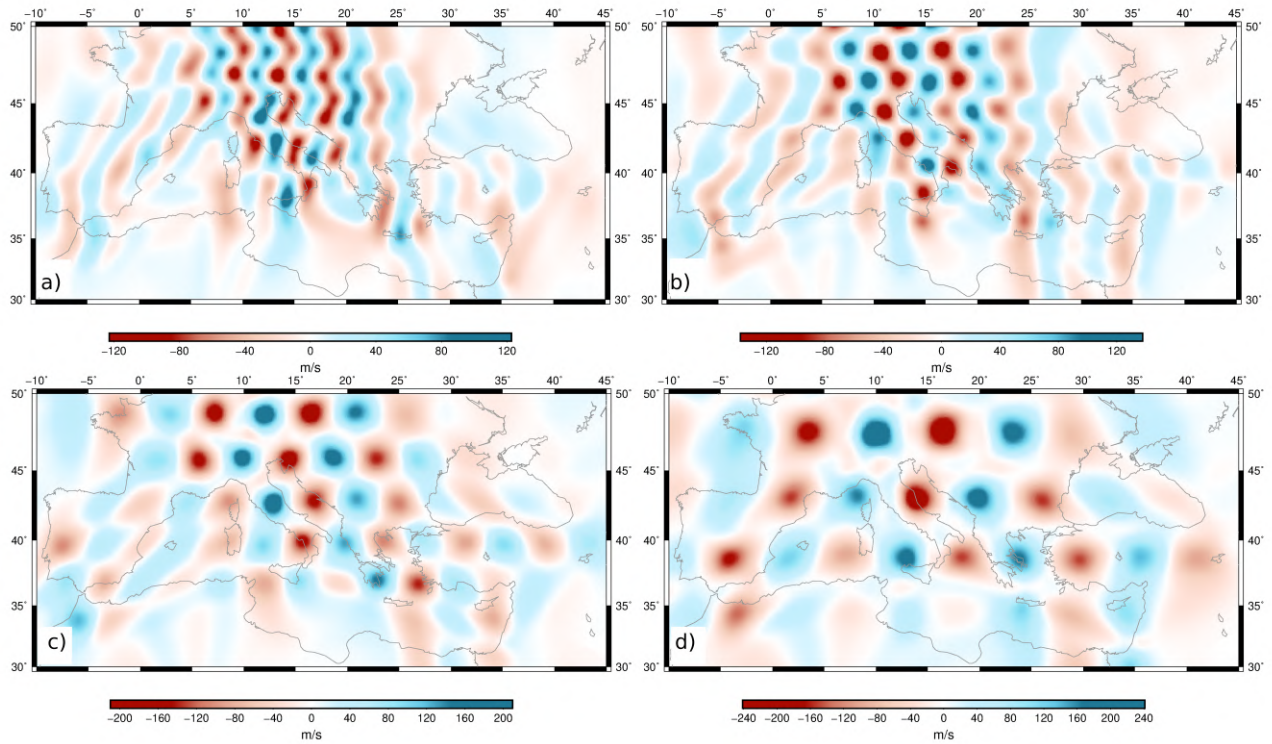
Figure S6.   Results of the checkerboard resolution tests at period of 100 s for a) 75 km, b) 100 km, c) 150 km and d) 200 km structure size.
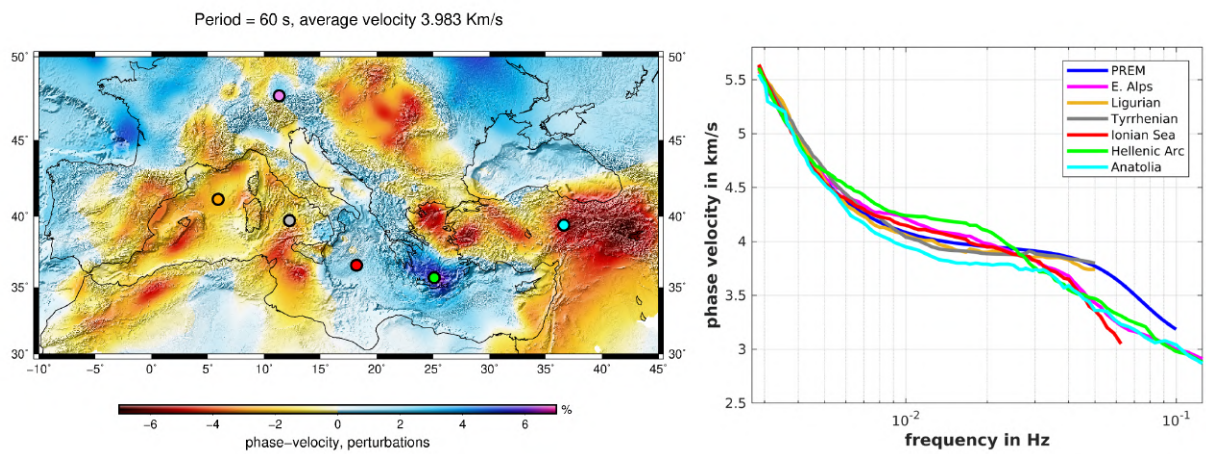
Figure S7.   Selected examples of the local dispersion curves as constructed from the phas-velocity maps. Their locations are indicated by circles in the phas-velocity map at period of 60 s.
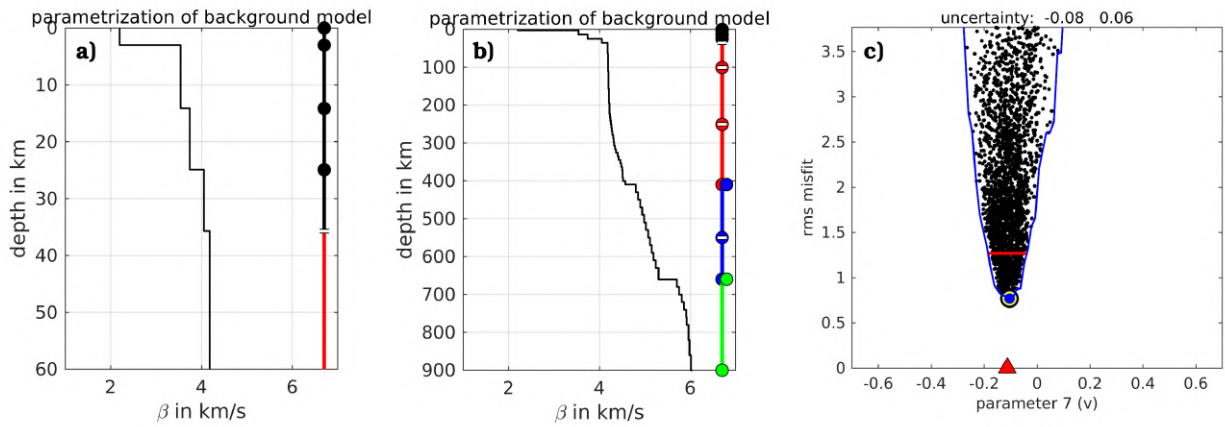
Figure S8. Graphical representation of the parameterization of the background model for the particle-swarm-optimization inversion. a) Parameterization of the crust taking into account the bathymetery. b) Full parameterization of the considered depth range including the crust, the upper mantle, the mantle transition zone and downwards to 900 km depth. The solid dots show the depth nodes where fixed discontinuities with variable velocities are considered, whereas white horizontal bars represent variable discontinuities. Constant perturbations of the shear-wave velocity of the background model are indicated by black line along the considered depth range. Green line indicates gradient perturbations, while blue and red line segments represent quadratic and cubic velocity perturbations respectively. c) A plot showing the determination of uncertainties of one model parameter (uppermost mantle velocity). They are plotted as function of the rms misfit values. Each black dot represents a single model of the tested range of models. The blue line define the envelope that contains the tested models. The outlined blue circle indicates the model with the lowest misfit. The red line defines the maximum allowed misfit for defining the model uncertainties. The red triangle indicated the centroid model.
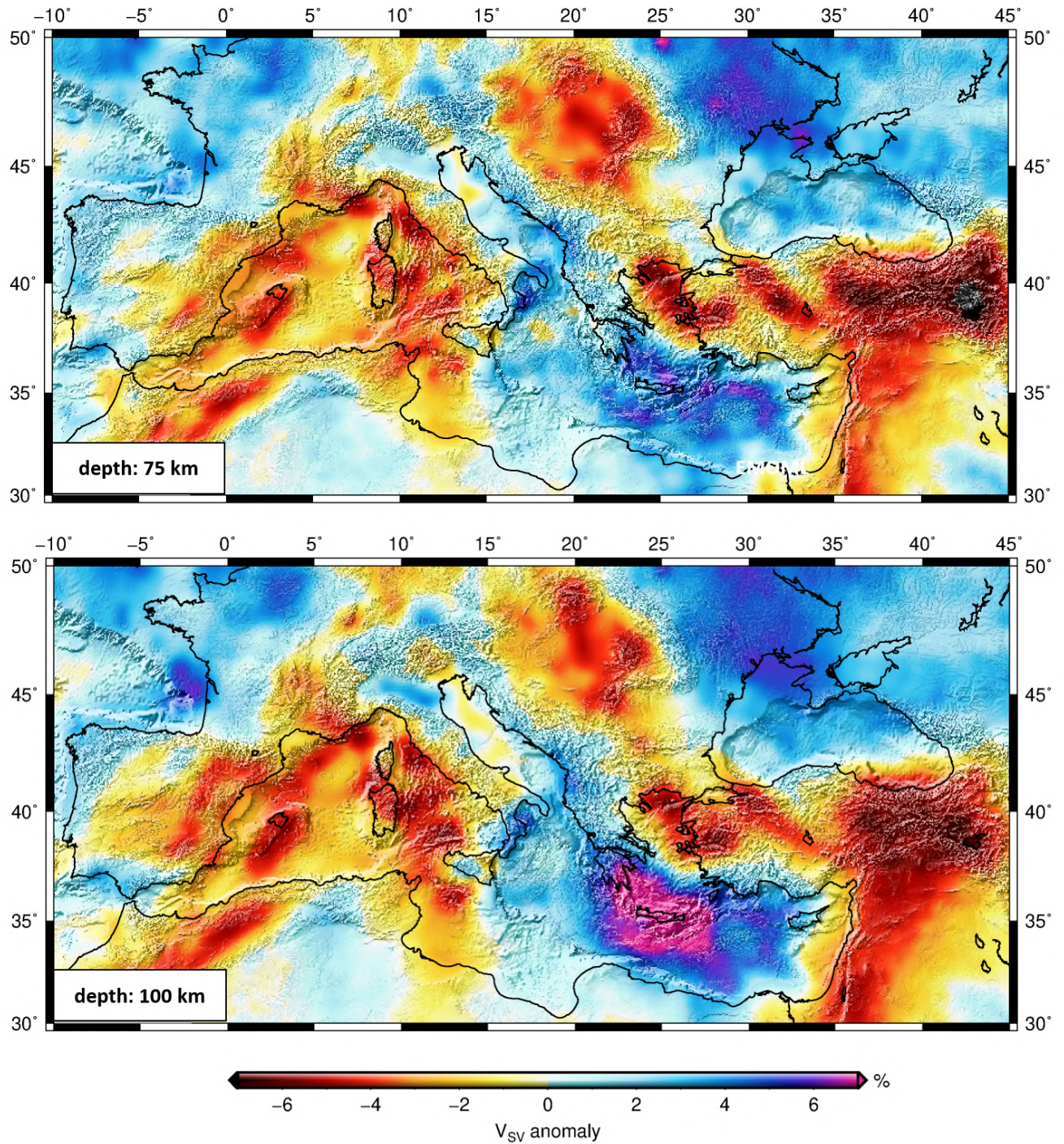
Figure S9. Horizontal map views of the 3-D shear-wave velocity model (MeRE2020) at 75 km and 100 km depth. The same maps as in Fig. 6 in the manuscript but without the annotations.
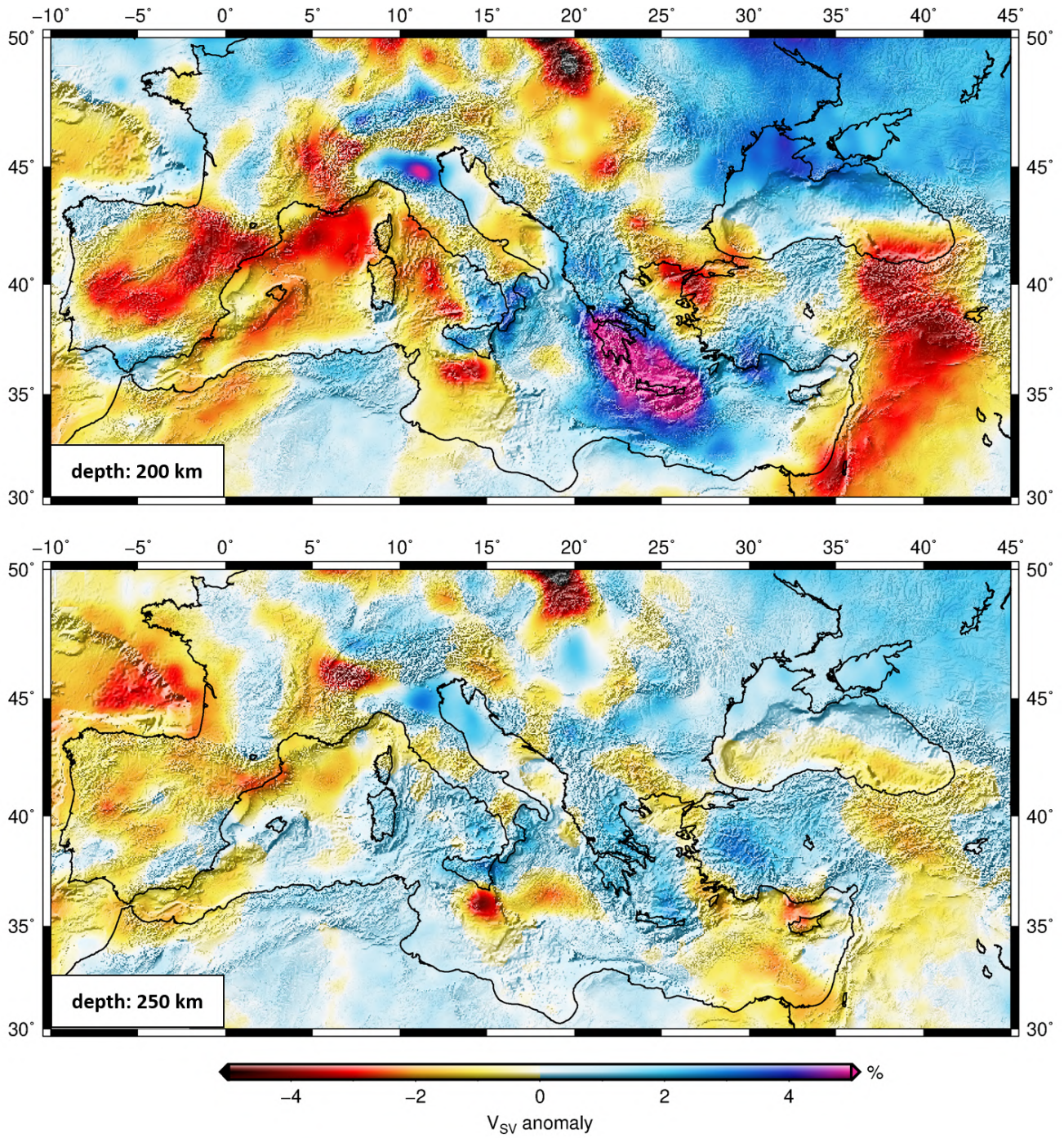
June 15, 2020, 8:18am

Figure S10.   Horizontal map views of MeRE2020 at 200 km and 250 km depth. The same maps as in Fig. 7 in the manuscript but without the annotations.
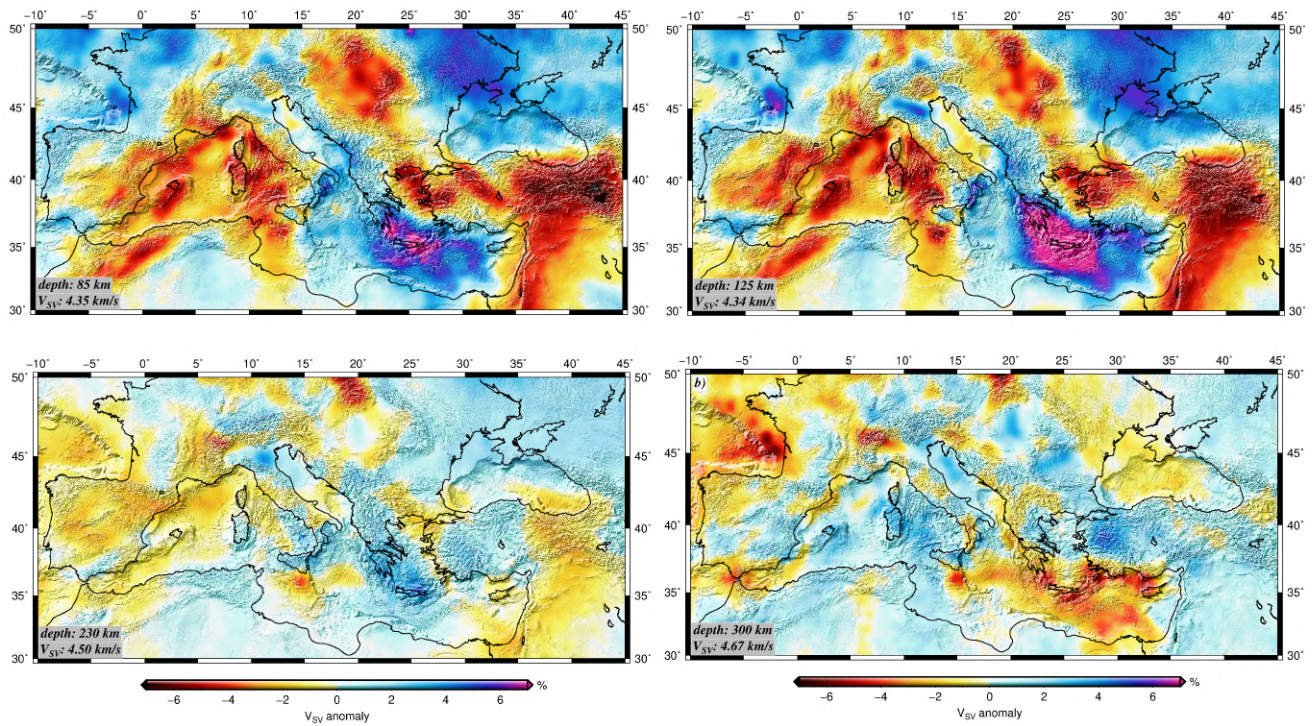
Figure S11.   Horizontal map views through MeRE2020 at 85 km, 125 km, 230 km and 300 km depth. Shear-wave velocity perturbations are shown with respect to a depth-dependent 1-D shear-wave velocity model indicated in Fig. 8.
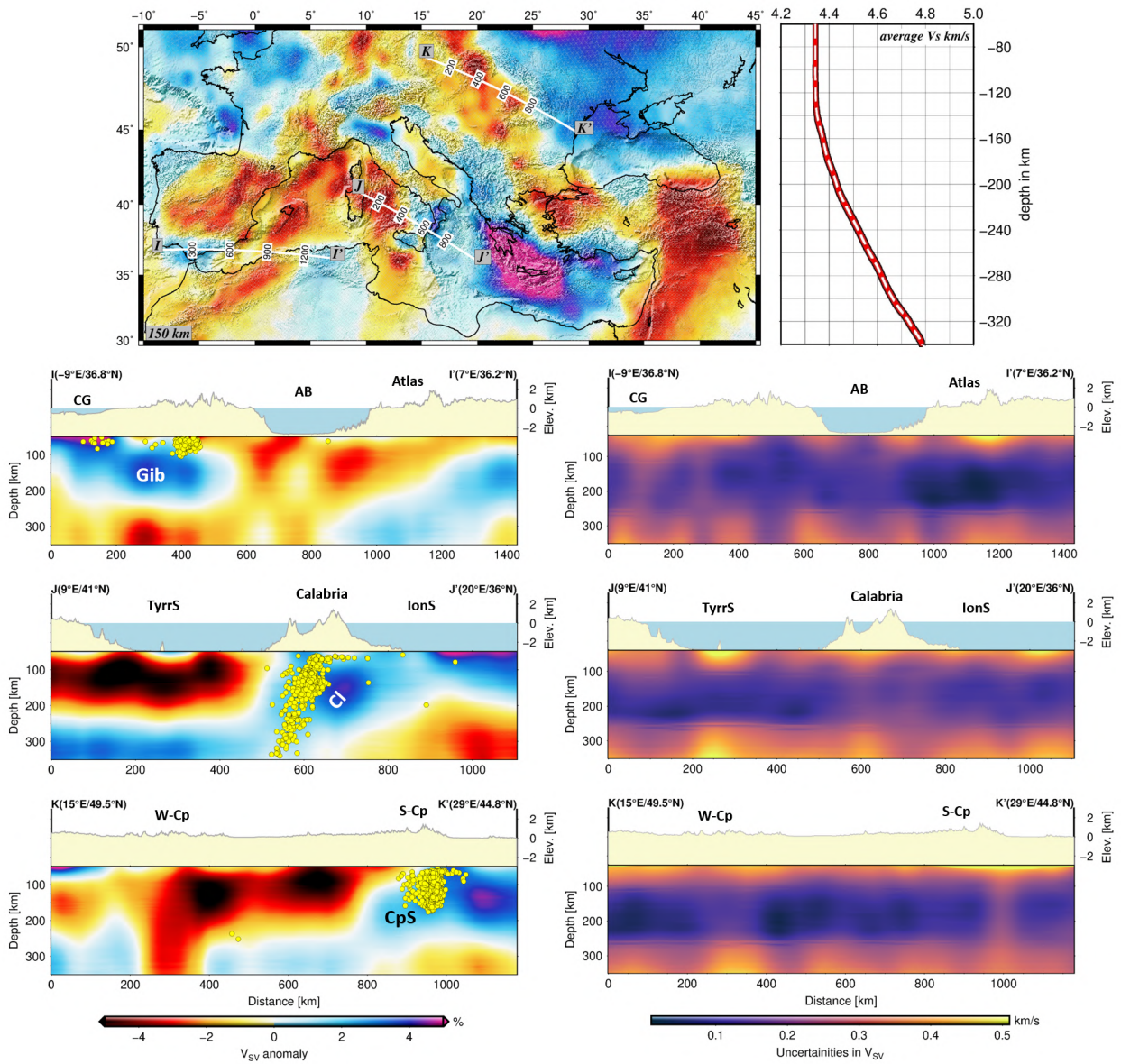
Figure S12. Vertical cross sections through MeRE2020 crossing a) the Gibraltar Slab, b) the Calabrian subduction zone and c) the Vrancea zone. Their locations are shown on the map at 150 km depth. Yellow circles define the intermediate-depth seismicity from the ISC catalogue (1990 - 2019) along these profiles. The depth-dependent uncertainties in MeRE2012 are plotted on the right hand side along the same profiles. AB: Algerian Basin, Cl: Calabrian Slab, CG: Gulf of Cadiz, CpS: Southern Carpathian Slab, Gib: Gibraltar Slab, IonS: Ionian Sea, Kb: Kabylides Slab, S-Cp: Southern Carpathians Mountains, TyrrS: Tyrrhenian Sea, W-Cp: Western Carpathians Mountains.

June 15, 2020, 8:18am